Received: 20 August 2024 | Revised: 3 December 2024 | Accepted: 20 December 2024

DOI: 10.1111/jne.13490

ORIGINAL ARTICLE

Journal of Neuroendocrinology WILEY

Capillary connections between sensory circumventricular organs and adjacent parenchyma enable local volume transmission

Yifan Yao[1] | Yannan Chen[2,3] | Raju Tomer[2,3,4] | Rae Silver[1,4,5,6]

[1]Department of Psychology, Columbia University, New York, New York, USA

[2]Department of Biological Sciences, Columbia University, New York, New York, USA

[3]Department of Biomedical Engineering, Columbia University, New York, New York, USA

[4]Zuckerman Institute, Columbia University, New York, New York, USA

[5]Department of Neuroscience, Barnard College, New York, New York, USA

[6]Department of Pathology and Cell Biology, Columbia University Medical School, New York, New York, USA

Correspondence
Rae Silver, Department of Psychology, Columbia University, New York, NY, USA.
Email: rae.silver@columbia.edu

Funding information
National Institutes of Health, Grant/Award Numbers: 1S10OD023587-01, DP2MH119423, R21NS134228; National Science Foundation, Grant/Award Number: 1749500

Abstract

Among contributors to diffusible signaling are portal systems which join two capillary beds through connecting veins. Portal systems allow diffusible signals to be transported in high concentrations directly from one capillary bed to the other without dilution in the systemic circulation. Two portal systems have been identified in the brain. The first was discovered almost a century ago and connects the median eminence to the anterior pituitary gland. The second was discovered a few years ago and links the suprachiasmatic nucleus to the organum vasculosum of the lamina terminalis, a sensory circumventricular organ (CVO). Sensory CVOs bear neuronal receptors for sensing signals in the fluid milieu. They line the surface of brain ventricles and bear fenestrated capillaries thereby lacking blood–brain barriers. It is not known whether the other sensory CVOs, namely the subfornical organ (SFO), and area postrema (AP) form portal neurovascular connections with nearby parenchymal tissue. To preserve the integrity of the vasculature of CVOs and their adjacent neuropil, we combined iDISCO clearing and light-sheet microscopy to acquire volumetric images of blood vessels and traced the vasculature in two experiments. In the first, the whole brain vasculature was registered to the Allen Brain Atlas in order to identify the nuclei to which the SFO and AP are attached. In the second study, regionally specified immunolabeling was used to identify the attachment sites and vascular connections between the AP, and the SFO to their respective parenchymal attachment sites. There are venous portal pathways linking the capillary vessels of the SFO and the posterior septal nuclei, namely the septofimbrial nucleus and the triangular nucleus of the septum. Unlike the arrangement of portal vessels, the AP and the nucleus of the solitary tract share a common capillary bed. Taken together, the results reveal that all three sensory CVOs bear direct capillary connections to adjacent neuropil, providing a direct route for diffusible signals to travel from their source to their targets.

KEYWORDS
area postrema, choroid plexus, diffusible signal, portal system, subfornical organ

1 | INTRODUCTION

With the increased understanding of volume transmission (VT) mechanisms,[1] the discovery of the glymphatic system,[2] and the distinct role of chemical secretions in modulating neural wiring networks,[3] it is clear that fluid systems of the brain, including the cerebrospinal fluid (CSF) and perivascular spaces are key players in central nervous system function and dysfunction.[4,5] Among the important elements are circumventricular organs (CVOs), a group of structures lining the surface of the ventricles. They have large perivascular spaces, are in contact with CSF, are highly vascularized, and most feature fenestrated capillaries, as reviewed in Ref. 6. These properties have led to the concept of CVOs as "windows of the brains."[7] CVOs are categorized into two groups—secretory and sensory.[6] The sensory CVOs include the organum vasculosum of the lamina terminalis (OVLT), subfornical organ (SFO), and area postrema (AP). They contain neurons expressing a wide variety of receptors to blood-borne signals, CSF contents, or neural inputs to relay sensed changes in fluid milieu to other regions of the brain, further modulating behavior and physiology.[8,9]

It is now known that there is a venous portal pathway connecting the capillary beds of the suprachiasmatic nucleus (SCN) to those of the OVLT.[10,11] However, whether each of the other sensory CVOs connects to the nearby parenchyma via a portal pathway remains unclear. In the literature on the vascular anatomy of sensory CVOs, there are suggestions of joined capillary beds between the other sensory CVOs and their respective adjacent parenchyma. Thus, Akert in 1969[12] commented on densely packed SFO capillary loops, and wrote, "It seems that the next step would consist in the intravital study of blood flow with special attention to the question of a portal circulation in the direction of the certain hypothalamic and septal areas." Roth and Yamamoto in 1968[13] reported that "two distinctively different capillary beds, one in the AP and the other in the medulla, are seen to be joined by short interconnecting vessels." Although the vasculature connection between the SFO, AP and their respective neighboring parenchyma is not clear, the anatomical localization of these regions have been described in several species, including mice (reviewed in Ref. 14–16). The SFO is located along the anterior-dorsal wall of the third ventricle (3V), where it lies at the dorsal extremity of the lamina terminalis. It is apposed to the ventral hippocampal commissure (VHC), is separated from the septal area by the VHC and extends into the lumen of the 3V where it lies adjacent to the choroid plexus (ChP) near the ceiling of the 3V.[14] The AP resides on the floor of the fourth ventricle (4V) and is attached to the nucleus of the solitary tract (NTS) at its ventral surface.

Portal systems in the brain are key to integrating brain and bodily functions. They are vascular arrangements where two capillary beds are linked by connecting veins.[17] Portal pathways enable blood-borne substances to be transported in high concentrations from the capillary bed of one region to the capillary bed of a local target site without dilution in the systemic blood supply.[17] The pituitary portal system was first identified almost 100 years ago.[18,19] Here, portal veins connect the capillary beds of the median eminence (ME) to those of the anterior pituitary gland. Hypothalamic-releasing hormones from the ME travel in the portal veins lying in the pituitary stalk to reach the capillary bed of the anterior pituitary gland. In the anterior pituitary gland, hypothalamic-releasing hormones stimulate the production of the pituitary trophic hormones, including the adrenocorticotropic hormone, thyroid-stimulating hormone, luteinizing hormone, and follicle-stimulating hormone to further regulate body wide behaviors.[20] For example, the portal pathway enables a small population of about 600 GnRH neurons are sufficient to support reproductive responses.[21] In this way, the pituitary portal system, via the pituitary gland, serves as a relay, amplifying signals from a small population of hypothalamic neurons to impact body-wide functions necessary for survival, including stress responses, reproduction, and metabolism.[22–25] The SCN, like the pituitary gland, has a body-wide impact.[26,27] This small nucleus serves as a daily clock which sets the phase of rhythms in "clock cells" throughout the body.[28–30] The SCN has both neural and vascular-portal connections to the OVLT[10,31] and the OVLT in turn, has extensive neural and vascular connections to the rest of the brain.[6,32,33] The foregoing evidence highlights the possibility that sensory CVOs are positioned to amplify neurosecretory signals from small populations of hypothalamic neurons.

Though the vasculature of SFO and AP have been described previously, capillary blood vessels (BVs) and connections to adjacent parenchyma and those to the ChP have not been examined. Our goal was to examine the capillary vasculature organization of the SFO and AP in relation to the parenchymal tissue and the ChP to which they are attached using a preparation that enables studying intact BVs and does not require tissue sectioning. We scanned iDISCO-cleared whole mouse brain vasculature using light sheet microscopy and immunochemistry for collagen to label the entire vasculature. We then conducted brain registration aligned to the Allen Mouse Brain Atlas (ABA) and computer-aided BV tracing to localize the capillary connections between SFO and AP and their adjacent brain regions, respectively. To test the findings more directly, we next examined the capillary organization of the regions that had been identified in the registered results in a separate series, using brain region-specific markers to definitively delineate SFO, AP, their adjacent parenchyma and their capillary networks.

2 | METHODS

2.1 | Terminology

We adopted the nomenclature of ABA[34] (Allen Institute for Brain Science, 2004) or Paxinos and Franklin's The Mouse Brain in Stereotaxic Coordinates[35] in describing the brain regions studied herein.

2.2 | Animals and housing

Male C3H mice ($n = 4$) and C57BL/6J mice ($n = 4$) aged 8–10 weeks were purchased from the Jackson Laboratory (Sacramento, CA). C3H

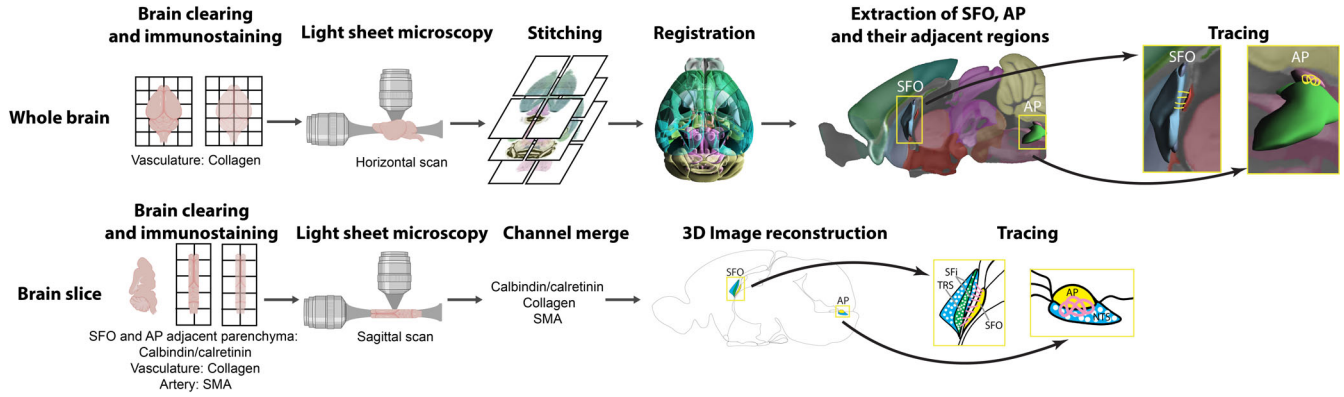

FIGURE 1 Experimental pipeline. Top row: procedure for whole brain clearing, imaging, and vascular connection analysis. Bottom row, procedure for brain slice (4 mm) clearing, imaging, and vascular connection analysis. AP, area postrema; NTS, nucleus of solitary tract; SFi, septofimbrial nucleus; SFO, subfornical organ; SMA, smooth muscle actin; TRS, triangular nucleus of septum.

mice were used for whole brain imaging and vasculature registration and C57BL/6J were used for brain slices for labeling specific nuclei. No strain differences were noted on the questions addressed here. C3H mice produce melatonin in the pineal gland,[36] while the more commonly used C57BL/6J animals do not. The mice were housed in the lab for at least 2 weeks after arrival prior to being used in these studies. All animals were provided with ad libitum access to food and water and maintained in a 12:12-h light: dark (LD) cycle (lights-on at 7:00 AM, where zeitgeber time (ZT) 0 refers to the time of lights on). All experiments were carried out in accordance with the guidelines of Columbia University's Institutional Animal Care and Use Committee protocol number AC-AABH1603.

2.3 | Perfusion

At ZT6 animals were deeply anesthetized (11%ketamine + 2%xylazine, 10 mL/kg body weight i.p.) and perfused intracardially with 50 mL 0.9% saline followed by 100 mL 4% paraformaldehyde (PFA) in 0.1 M phosphate buffer (PB), pH 7.3. Brains were post-fixed at 4°C overnight. The next day, brains for iDISCO were washed with PBS and stored in PBS with 0.02% sodium azide at 4°C until future use.

2.4 | Brain clearing and immunostaining for whole brain and brain slices

The experimental pipeline is shown in Figure 1. For both the whole brains of C3H mouse and brain slices of C57BL/6J mouse, the iDISCO protocol was used[37] with the following modifications. For whole brain analysis, primary antibody goat anti-type IV Collagen-UNLB (1:50, SouthernBiotech, 1340-01, LOT H2915-PI54, Birmingham, AL) was used to label the entire vasculature and secondary antibody donkey anti-goat Cy5 (1:200, Jackson ImmunoResearch) was used to identify collagen. Brains were incubated with the primary antibody for 2 weeks followed by the secondary antibody for 1 week.

To preserve midline CVOs and their nearby regions brain slices were prepared in the sagittal plane with 2 mm of tissue on each side of the midline with a steel brain matrix (Ted Pella, Redding, CA). The primary antibody solutions were mouse anti-smooth muscle actin (SMA) antibody (1:67, Dako, M0851, LOT 41480056, Santa Clara, CA) for labeling arteries and goat anti-collagen (as above) for labeling the entire vasculature. A mixture of rabbit anti-calretinin (1:500, Chemicon, AB149, LOT 25797041, Temecula, CA) and rabbit anti-calbindin (1:5000, Swant, CB38a, Burgdorf, Switzerland LOT 9.03) to identify hypothalamic and brainstem regions adjacent to the SFO and AP.[38,39] Secondary antibodies were as follows: for calretinin and calbindin, donkey anti-rabbit Cy2 (1:200, Jackson ImmunoResearch); for SMA, donkey anti-mouse Cy3 (1:200, Jackson ImmunoResearch); for collagen, donkey anti-goat Cy5 (1:200, Jackson ImmunoResearch). Tissues were incubated with primary antibodies for 1 week and then with secondary antibodies for 4 days.

2.5 | Light-sheet microscopy

Whole brain samples were imaged using CLARITY-Optimized Light Sheet Microscopy (COLM) as previously described.[40] An Olympus 10× objective was used and achieved a pixel size of 0.585 µm, with further downsampling applied for efficient processing. The image tiles were stitched using BigStitcher[41] with a careful manual inspection to ensure vasculature connectivity.

For brain slices, images were acquired with Ultramicroscope II (LaVision BioTec, Bielefeld, Germany) equipped with an Olympus MVX10 zoom body (Olympus, Barlett, TN), a LaVision BioTec Laser Module (LaVision BioTec), and an Andor Neo sCMOS Camera (Andor Technology, Concord, MA) with camera sensor pixel size of 6.5 µm. The following lasers and filters were used: Cy2-calretinin/calbindin was excited at 488 nm and emission was acquired at 525 ± 50 nm; Cy3-SMA was excited at 561 nm and acquired by 605 ± 50 nm; Cy5-collagen was excited at 639 nm and emission was collected at 705 ± 72 nm. The vasculature of the SFO and the AP regions were

scanned horizontally with a voxel size of 0.94 × 0.94 × 1 μm (left–right × rostral-caudal × dorsal-ventral).

2.6 | Whole brain registration

The whole brain samples were aligned using suiteWB pipeline[42] as previously described. Specifically, suiteWB employs a multi-step multi-resolution 3D registration approach using Mutual Information as the similarity metric. The registration process initiates with a rigid transformation, incorporating six degrees of freedom for rotation and translation, aligning the moving image (i.e., the image being aligned) roughly with the reference image. Subsequently, the moving image undergoes an affine transformation involving 12 degrees of freedom to address shearing and shrinking artifacts introduced during labeling, tissue clearing, and imaging. Finally, a uniform grid of control points and third-order B-splines are used to account for non-rigid local transformations. Affine and nonrigid steps were executed at three different resolutions. The algorithms were implemented with ITKv4.[43] All samples underwent registration using a 488 nm channel onto our local average reference brain at 10 μm resolution with corresponding ABA brain region annotations, and the resultant spatial transformation parameters were applied to high-resolution datasets with a lateral resolution of 2.5 μm and axial resolution of 5 μm.

2.7 | Extraction of CVOs and neighboring regions

CVOs were initially identified using the ABA brain region annotations, and neighboring regions were chosen based on the 8th level of the ABA hierarchy tree, encompassing areas within a 25 μm distance of the CVO bounding box. Subsequently, a cubic region of interest (ROI) with edges measuring 1250 μm was cropped, centered on the CVO, to facilitate detailed manual inspection and tracing. The alignment between the ABA annotation mask and the brain within the ROI was further refined manually through translation and rotation adjustments.

2.8 | Tracing

Acquired samples were imported into Imaris (Bitplane AG, Zurich, Switzerland) for tracing. Tracing was done with the "filament" model in the collagen-labeled channel. The autodepth mode was used with auto-center and auto-diameter correction.

2.9 | BV diameter measurement and statistical analysis

The outer diameter of capillary vessels was measured in BV segments of septofimbrial nucleus (SFi) and triangular nucleus of septum (TRS), AP, NTS and SFO. In addition, portal vessel diameters were assessed.

Five BV segments of each type were randomly chosen from light sheet images of C57BL/6J mice ($N = 4$). The outer diameter was measured with the "Straight" line tool in Fiji ImageJ.[44] The capillaries were identified as BV segments that have diameters below 10 μm which doesn't have intense and continuous SMA staining, as veins and venules have weaker and more sporadic staining of SMA than arteries and arterioles.[45] SFO portal vessels are identified by their location as the intervening vessel between the two capillary beds of SFO and the adjacent posterior septal nuclei. Capillaries of AP and its neighboring NTS are differentiated by distinct collagen staining intensity in either region, where AP has stronger staining than NTS (original measurements are documented in Supplementary Table S1). All groups of diameter measurements are normally distributed and establish sphericity (Supplementary Table S2). The comparison of CVO capillaries, portal vessel and capillaries in the adjacent parenchyma was done with repeated measurement ANOVA, followed by post-hoc multiple pairwise comparisons with Benjamini/Hochberg FDR correction. All statistical analyses were done with Python 3.0 and its packages NumPy,[46] Pandas,[47] and Pingouin.[48] Graphs were created with Python packages Matplotlib[49] and Seaborn.[50]

3 | RESULTS

3.1 | Vascular connections between SFO and adjacent parenchyma in iDISCO cleared, registered brain

The rostral SFO lies near the TRS and SFi, but is separated from these nuclei by the ventromedial hippocampal commissure (VHC, Figure 2A–D). The TRS and SFi together, have been described as the posterior septal nuclei.[51,52] As seen in the collagen-labeled vasculature registered to the ABA, the dorsal, caudal, and ventral aspects of the SFO protrude into the 3V (Figure 2E, sagittal view). Our whole brain registration material suggests that the rostral SFO is attached to the VHC whose upper 4/5th abuts the SFI and its lower 1/5th abuts the TRS.

In the SFO, shown in sagittal, horizontal, and coronal orientations, BVs identified by collagen labeling form an intensely tangled web that protrudes into the 3V (Figure 2E, left panel). In contrast, the BVs lying rostral to the SFO, encompassing the posterior septal nuclei, are sparser. In the sagittal view of SFO, the collagen-labeled and the traced BVs indicate that several vessel segments emerge from SFO capillaries along its entire dorsoventral axis (Figure 2E, top row). In the upper 4/5th where the VHC lies between the SFO and SFi, the BV segments penetrate the VHC, and first arborize into capillaries in the SFi and then further arborize in the TRS. In the lower 1/5th of the SFO, where the ventral VHC directly contacts the TRS, the BV segments emerging from the bottom of the SFO directly enter the TRS (Figure 2E, top row). In the horizontal and the coronal view (Figure 2E, middle and bottom row), the vascular connection between the SFO capillaries and those in the posterior septal nuclei can also be

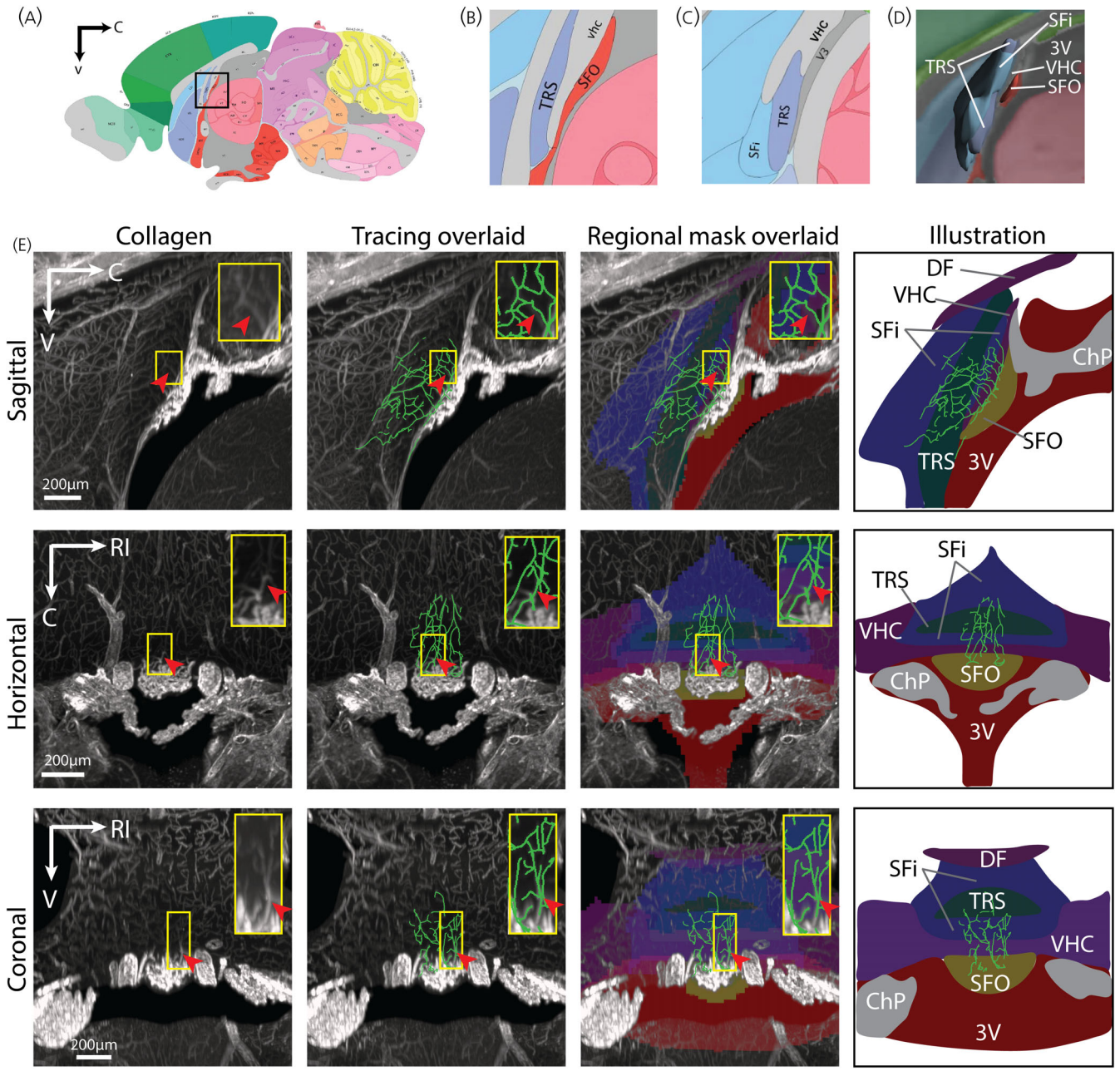

FIGURE 2 Vasculature of SFO and adjacent parenchymal region using the ABA for Registration. (A) Schematic of the brain (P56 sagittal view #20[34]) in sagittal view; the boxed area demarcates the region containing the SFO. (B) Magnified view of the boxed area of (A). (C) Magnified view of region lateral to b showing the spatial relationship between TRS and SFi (P56 sagittal view #17 in ABA). SFO is not present at a locus. (D) 3D atlas view (ABA) enabling a view of SFi, TRS, VHC, and 3V, all regions adjacent to the SFO. (E) Vascular connections between SFO and the SFi and TRS regions in sagittal (upper row), horizontal (middle row) and coronal (lower row) orientations. Depicted from left to right: Collagen labeling of the vasculature of the SFO and its nearby regions, tracing overlaid on vasculature staining, registered regional masks merged with traces and vasculature, and a summary illustration. Insets highlight vascular connections (arrowheads) between the SFO and the posterior septal nuclei (which encompasses both SFi and TRS). $z = 100$ µm. Color code: ChP = gray; DF and VHC = dark purple; SFi = dark blue; SFO = dark yellow; TRS = dark green; 3V = dark red. ABA, Allen mouse brain atlas; C, caudal; ChP, choroid plexus; DF, dorsal fornix; LE, left; RI, right; V, ventral; VHC, ventral hippocampal commissure; 3V, third ventricle. The remaining abbreviations as in Figure 1.

seen along the mediolateral axes of these nuclei. It remains to be determined whether these are connecting venules or direct capillary connections. It also remains to be proven that the registered material correctly identifies the brain regions. In order to further characterize the BV connections between the SFO and the posterior septal nuclei, we next identified the SFi and TRS using immunostaining.

3.2 | Vascular connections between SFO and adjacent parenchyma in iDISCO cleared immunostained brain sections

The immunostaining results indicate that the size of calbindin/calretinin stained neurons in SFi are larger than those in TRS, consistent with previous reports that the SFi contains "septal giant cells" (15–21 μm, scattered), whereas those in the TRS have a relatively smaller size (7–14 μm, densely packed).[51,53] The localization of these nuclei confirms the results seen in brains registered to the ABA showing that VHC lies between the SFO and the posterior septal nuclei (Figure 3A). Importantly, several BV segments emerge from the SFO along its rostral surface and traverse the VHC (Figure 3B). At its upper 4/5th of the VHC attached to SFO, the portal vessels branch to join the capillaries of SFi (Figure 3C,D). At the lower 1/5th, the portal vessels first travel ventrally and then arborize and connect to the

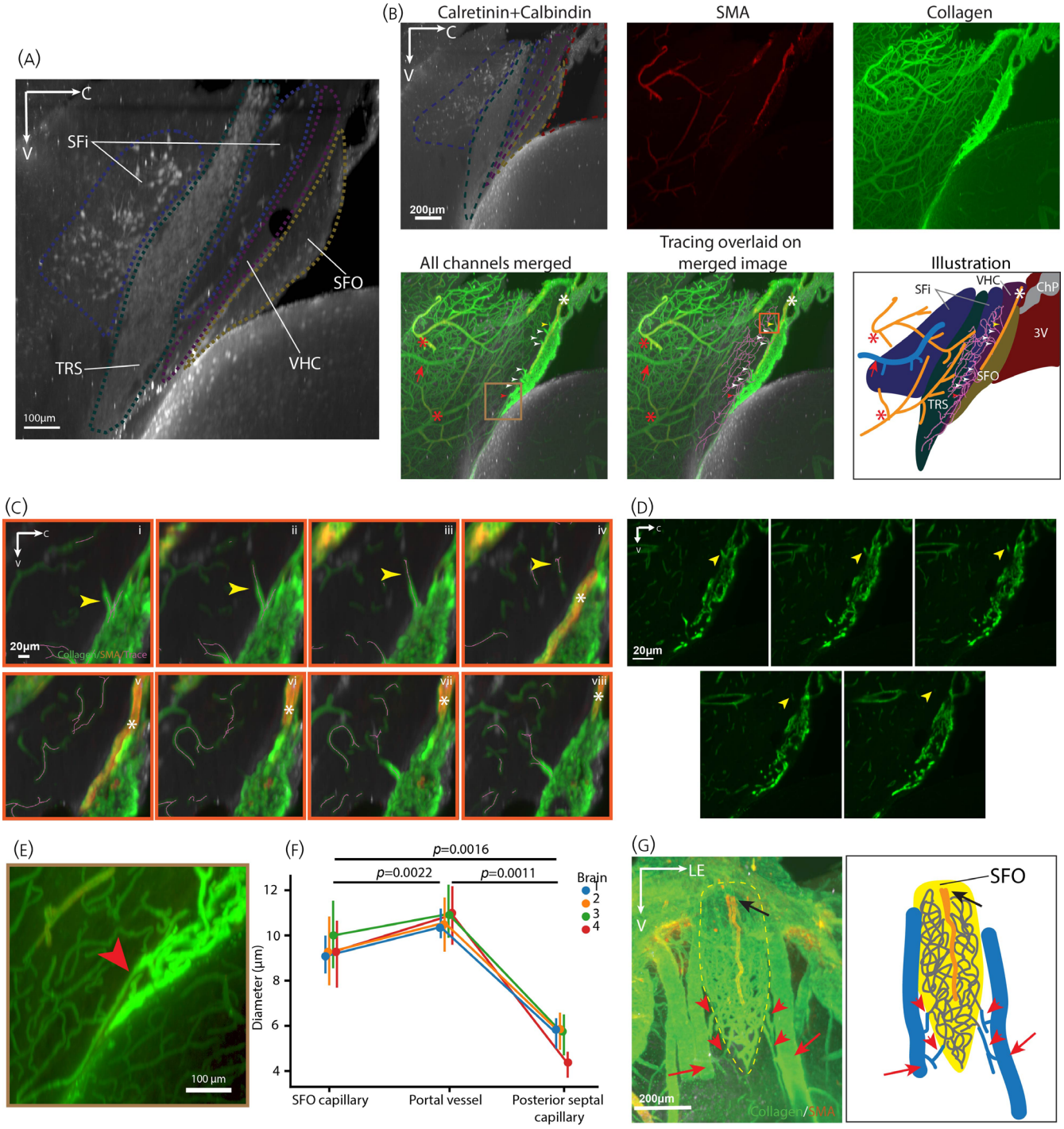

FIGURE 3 Legend on next page.

capillaries of the TRS and connect to the capillaries of the SFi and TRS (Figure 3E). The trunks of these portal venules are BV segments that bear no branch points.

As is typical of portal venules, the diameter of the portal venules penetrating the VHC is significantly larger than the capillaries in either the SFO or the posterior septal nuclei (Figure 3F). The diameters of SFO and posterior septal capillaries and connecting portal vessels were as follows: SFO (9.42 ± 1.61 μm), portal vessels (10.70 ± 1.31 μm), and posterior septum (5.33 ± 1.02 μm). Statistical analysis was performed using repeated measurement ANOVA ($F_{(2,6)} = 140.2720$, $p = 9.1808 \times 10^{-6}$) followed by post-hoc multiple pairwise comparisons with Benjamini/Hochberg FDR correction: SFO capillary versus portal vessel (uncorrected $p = .002229$, corrected $p = .002229$); SFO capillary versus posterior septal capillary (uncorrected $p = .001598$, corrected $p = .002229$); portal vessel versus posterior septal capillary (uncorrected $p = .001081$, corrected $p = .002229$). Data in the plot is shown as $\bar{x} \pm$ SD. Detailed statistical results are in Supplementary Table S2.

3.3 | Arterial supply and venous drainage of SFO and the posterior septal nuclei

The arteries and veins of the SFO and the posterior septal nuclei are clearly seen in the calbindin/calretinin labeled sample. In the sagittal view, the arterial supply of SFO enters its dorsal aspect and travels ventrally along the rostral surface of SFO, at the interface between SFO and the VHC (Figure 3B). In coronal view, the SFO artery travels along the midline, running dorsoventrally (Figure 3G), extending 2/3rd of the length of the dorsoventral axis of SFO. At its bottom 1/3rd, the SFO artery arborizes into arterioles and capillaries. The arteries supplying the posterior septal nuclei have two sources, as seen in the sagittal view. One enters the posterior septal region from its rostroventral aspect. The branches of this artery mostly extend caudally and vascularize the part of posterior septal neuropils closely attached to the VHC. The second artery supplying the posterior septal nuclei enters this region from its rostral aspect. Some arteriole branches of this artery arborize and then join the capillaries in the caudal part of the posterior septal nuclei. As seen in the coronal view, the draining veins of the SFO are a series of small veins formed on the lateral edges along its dorsoventral axis. They run either laterally or ventrally and then merge into the larger vein next to the SFO (Figure 3G). In sagittal view, it can be seen that the draining vein of the posterior septal nuclei collects the capillaries from the rostral region, in close apposition to its supplying artery (Figure 3B).

3.4 | Vascular connections between AP and adjacent parenchyma in iDISCO cleared, registered brain

We next examined AP and its neighboring regions in the registered sample (Figure 4A). As in prior work in several species,[54] we find that the AP is located at the caudal end of the 4V floor (Figure 4A,B). Its rostral aspect protrudes into the CSF. The ventral AP is in close contact with NTS, and the major volume of the AP is embedded in the latter. Of interest here is the capillary organization of the AP and NTS (Figure 4C). The AP and NTS capillaries can be distinguished by differences in the intensity of collagen staining, with much stronger collagen expression in AP BVs. In the sagittal view of the medial plane of the brain (Figure 4C, top row), the ventrocaudal part of the AP capillaries spread into the NTS. At its most rostral tip (arrow) capillaries of the AP are connected to the ChP in the 4V. In the horizontal and coronal view (Figure 4C, middle and bottom row), the capillaries of lateral AP merge into the surrounding NTS and the rostral AP is in contact with the wall of 4V. In the coronal view, capillaries in the ventrolateral

FIGURE 3 Vascular connections between SFO and posterior septal nuclei (TRS and SFi) in calbindin/calretinin immunostained sections. (A) The SFO abuts the VHC to its full extent, while the VHC abuts the SFi at its upper 4/5th, and the TRS at its lower 1/5th. Note that the SFi wraps around TRS. (B) SFO-posterior septal area vasculature labeled with vascular and neuronal markers are shown in the same brain seen in A. From left to right, the upper row shows the immunochemical delineation of the SFi and TRS regions, and the bottom row merges the immunostained channels, followed by panels showing blood vessel tracing and an illustration summarizing all these elements. Portal vessels (arrowheads) at the rostral aspect of the SFO penetrate the VHC and join the capillary vessels in the SFi and TRS. The artery supplying the SFO (white asterisk) enters from its dorsal aspect. Arteries supplying the posterior septal nuclei enter at the rostrodorsal and rostroventral aspects (red asterisk). The draining vein of the posterior septal nuclei leaves from its rostrodorsal aspect (red arrow). (C) Magnified views of a portal vessel (yellow arrowhead) in the orange boxed area shown in (B) in the panel labeled "tracing overlaid on the merged image." (i–iv) A portal vessel (yellow arrowhead) penetrates the VHC and connects the rostral SFO capillaries to those of the SFi, shown in serial 12 μm optical sections. (iv–viii) An artery (asterisk) supplying SFO lies above the point of emergence of the portal vessel, shown in serial sections. The artery lies ~12 μm above the portal vessel (iii vs. iv). (D) In order to confirm the point at which it enters the SFO, a portal vessel connecting to the capillary bed of the SFO shell was examined in greater detail (2 μm optical slices, every 5 μm). Yellow arrowheads point to the same portal vessel as in Figure 3C. (E) Magnified view of a portal vessel connecting SFO and TRS. (The red arrowhead in this panel and in the boxed area in the "all channels merged" panel in (B) point to the same blood vessel). A portal vessel (red arrowhead) travels ventrally before branching and joining the capillaries in the TRS. (F) Diameter ($\bar{x} \pm$ SD) of SFO and posterior septal capillaries and connecting portal vessels ($N = 4$ brains, 5 BV segments/category/brain). (G) Arterial supply and venous drainage of SFO. The supplying artery travels along the dorsoventral axis (black arrow) of the SFO, extending 2/3 of its length. Small veins form near the lateral edges of both sides of the SFO (red arrowheads) and then drain to larger veins (red arrows). (A, B, E) $z = 150$ μm; (C) $z = 12$ μm; (D) $z = 2$ μm; in (G) $z = 300$ μm. Color code: Arteries = orange; capillaries = gray; SFO = yellow; veins = blue. Abbreviations as in Figures 1 and 2.

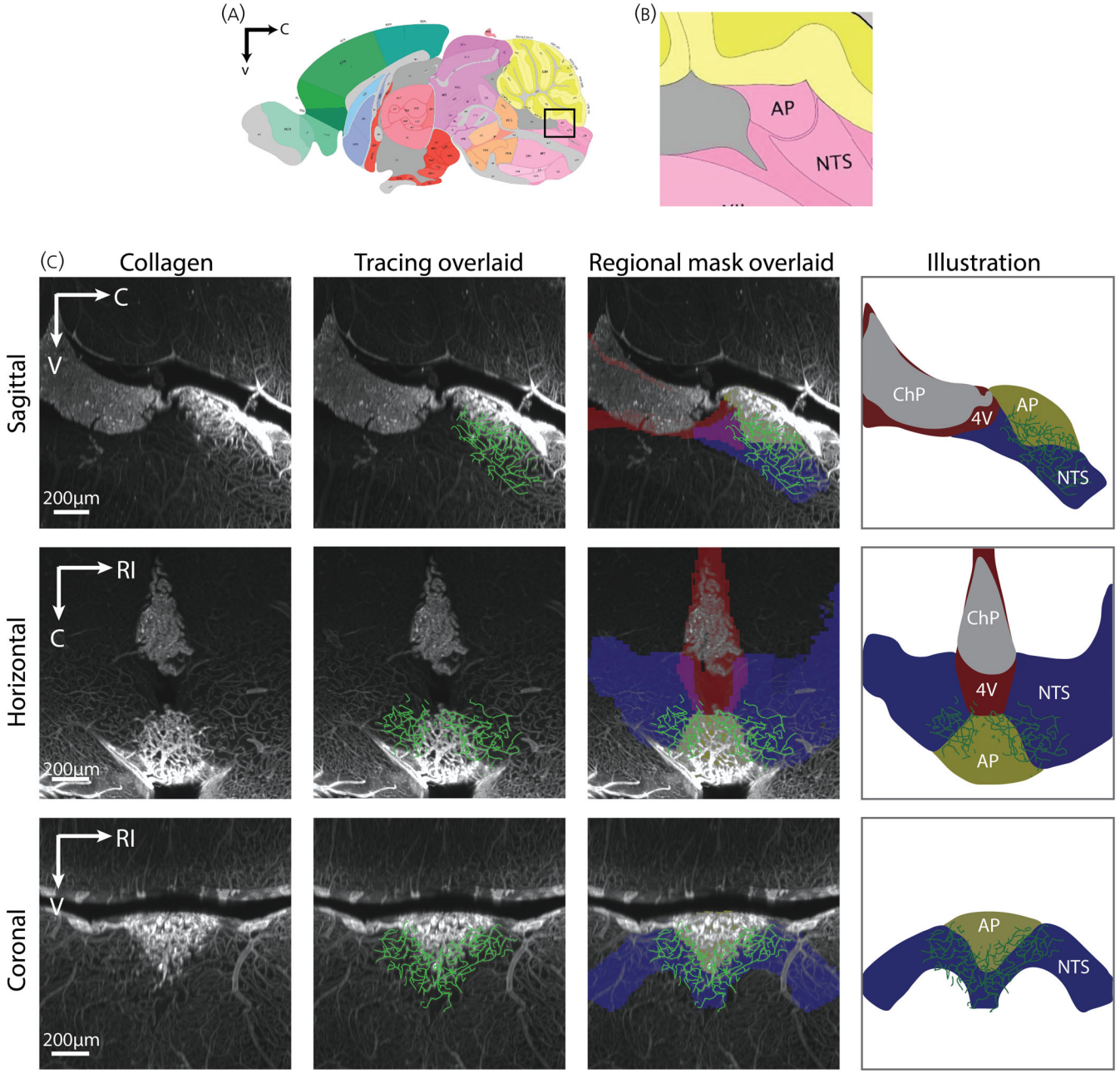

FIGURE 4 Identification of AP and Adjacent Parenchymal Vasculature using the ABA for Registration. (A) Schematic of the brain and the boxed area demarcating the region containing AP in the sagittal view. (Schematic from ABA). (B) Magnified view of the boxed region of (A). (C) Vascular connections between AP and NTS in sagittal (upper row), horizontal (middle row), and coronal (lower row) orientations. Depicted from left to right panels: Collagen labeling of the AP and its nearby vasculature, tracing overlaid on blood vessel staining, registered regional masks overlaid with traces and blood vessel staining, and a summary illustration. The shared capillary network of AP and NTS can be seen in all three orientations. $z = 150$ μm. Color code: AP = yellow; ChP = gray; NTS = blue; 4V = red. 4V, fourth ventricle. The remaining color codes and abbreviations as in Figures 1–3.

aspect of AP form web-like connection with the adjacent NTS. Tracing of the AP capillaries shows that they extend into ventral, lateral, and caudal directions and are continuous with the capillaries of the NTS (Figure 4C, regional mask overlaid on collagen labeled and traced vessels).

Next, calbindin and calretinin antibodies were used to definitively identify the NTS[38] in order to evaluate the precise relationships of the capillary vessels of the AP and NTS in this preparation. Calbindin/calretinin-positive cells are seen in the region adjacent to the AP in sagittal, horizontal, and coronal orientations (Figure 5A). The results indicate that the capillary vessels from the ventral surface of the AP extend into the NTS and merge with the NTS capillaries, seen in a high-power view at the interface of these regions (Figure 5B). The capillaries from both regions form a fully intertwined capillary network. The more intense

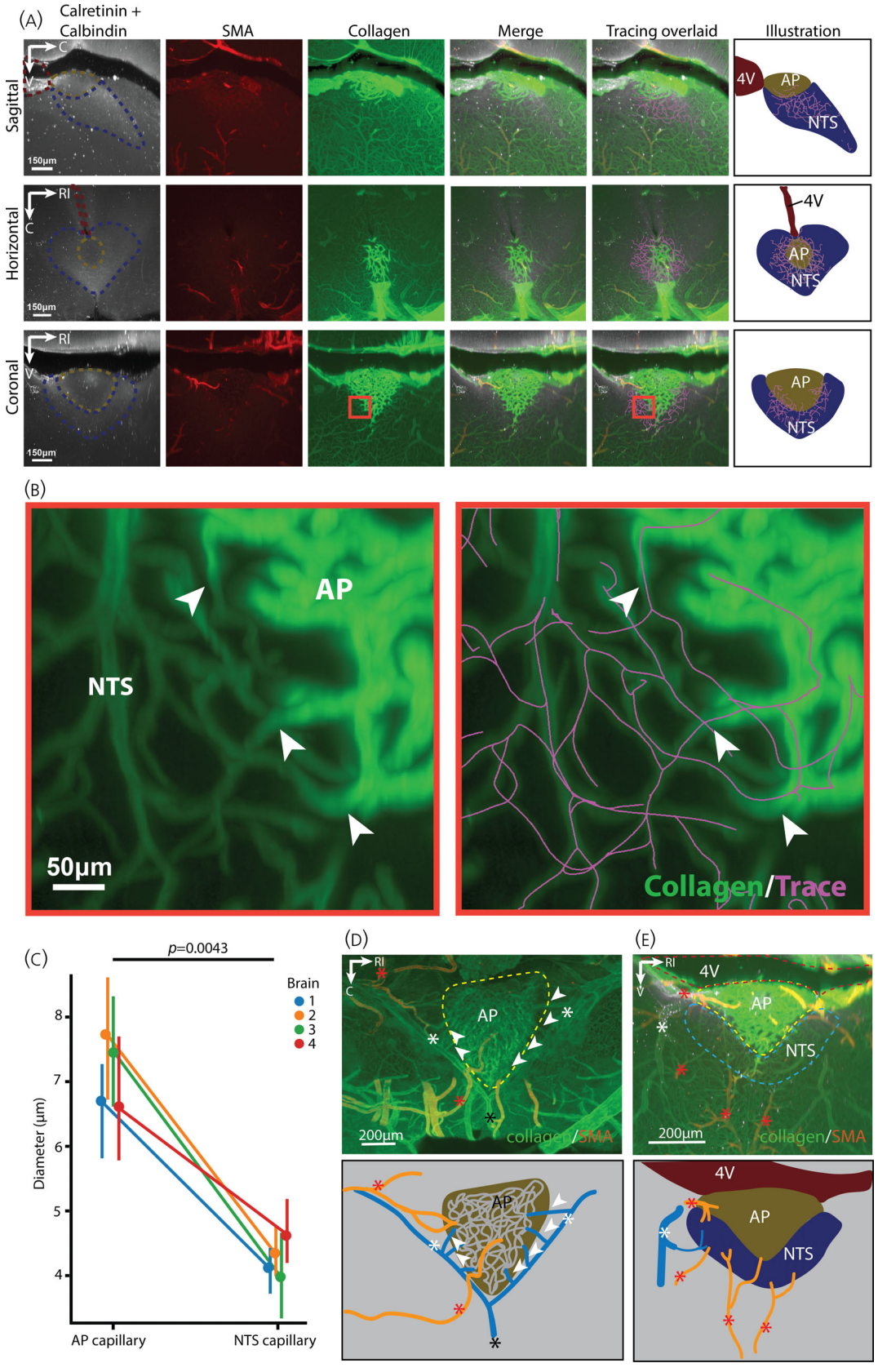

FIGURE 5 Legend on next page.

collagen signal in the AP capillaries compared to those of the NTS is due to the different sizes of capillaries in these two regions, with larger capillaries in the AP than in the NTS (Figure 5C).

3.5 | Arteries and veins of AP and NTS

AP and NTS share a joint capillary bed, but they have separate arterial supplies and venous drainage systems. As shown in the horizontal slice (Figure 5C), the artery supplying the AP comes from the lateral sides of the medulla and enters the AP from its caudal aspect. AP capillaries merge into a draining vein on each side. The two draining veins converge into a common vein which courses caudally. In the NTS, two supplying arteries can be seen in the coronal view (Figure 5D). One is the penetrating artery from the ventral medulla, entering the NTS from its ventral aspect. The other is the artery traveling along the dorsal surface of the medulla, entering NTS from its dorsal aspect. The NTS is drained by veins converging at its lateral and ventral aspect (Figure 5E).

3.6 | SFO and AP capillaries connections with the ChP

In addition to their connections with the parenchyma, SFO and AP capillaries also connect to the ChP (Figure 6). In the SFO, capillary branches exit the dorsal SFO and connect to the ChP capillaries (white arrowheads, Figure 6A) that lie near the roof of the 3V, as previously documented.[55,56] The AP capillaries run rostrally and join the ChP capillaries near the caudal 4V, as previously reported.[16]

4 | DISCUSSION

4.1 | Major findings

Shared capillary beds allow diffusible signals to travel from one brain nucleus to another without being diluted in the systemic vascular supply. Such local vascular pathways permit very small populations of neurons to produce secretions that impact specialized local targets. A portal system linking the SCN and the OVLT has previously been described, namely the SCN-OVLT portal system.[10] The present work raised the question of whether the other sensory CVOs, namely SFO and AP, share capillary bed connections with the neuropils to which they are attached, as this would provide a means for signals to course directly from one nucleus to the other.

The two major findings in the current study both demonstrate direct vascular connections between the capillary beds of the SFO and AP and the adjacent neuropil. The results indicate the surprising finding of a third portal system in the brain, namely venules joining the capillary beds of the SFO to that of the posterior septal nuclei. This arrangement meets the classical definition of a portal system—an arrangement of two capillary beds bearing vessels connected by intervening venules (termed portal veins).[17] In the other known portal systems in the brain, the capillary bed vessels are of smaller diameter than those of the portal venules.[11,57,58] In the current study, the portal vessels connecting the SFO and the posterior septal nuclei are also larger than the capillaries in both regions, consistent with findings in other identified portal systems (Figure 3F). The second major finding in the current study is that the capillary vessels of the AP connect directly to the capillary bed of NTS with no intervening portal veins. The finding that all three sensory CVOs in the mouse brain bear direct capillary connections to their adjacent parenchyma indicates a new route for local transmission of diffusible signals and a previously unknown pathway for VT.

4.2 | Relationship of present result to prior literature

Given the tremendous amount of research that has been done on the brain, it is surprising to find new anatomical pathways. Previous research on the whole brain vasculature often failed to report all or some CVOs.[59–63] For example, the BV mapping and analysis in different brain regions by Di Giovanna et al.,[59] Miyawaki et al.[62] and

FIGURE 5 Vascular connections between AP and NTS in calretinin/calbindin labeled brain slices. (A) Vasculature of AP and the NTS region in sagittal (upper row), horizontal (middle row), and coronal (lower row) orientations. For all rows from left to right, NTS labeled by calretinin/calbindin, arteries labeled by SMA, and vasculature labeled by collagen, a merge of calretinin/calbindin, SMA, and collagen, merge image overlaid with blood vessel tracing, and their illustration. The ventral, lateral, and caudal surfaces of the AP are covered by the NTS, and the rostral corner of the AP protrudes into the 4V. In all three orientations, the results indicate that the capillaries beds of AP and NTS are shared. Color coding as in Figure 4. (B) Magnified view of the boxed region in (A) bottom row third panel (left, collagen staining) and fifth panel (right, collagen merged with tracing). It shows at the border of AP and NTS, the capillaries of both regions form a shared network. Arrowheads point to locations of transitions of capillaries from AP to NTS. (C) Diameter of AP and NTS capillary vessels (four brains, five capillary segments in each region of each brain). The diameter ($\bar{x} \pm$ SD) of the AP and NTS capillaries are 7.12 ± 1.15 μm and 4.26 ± 0.61 μm respectively. Statistical analysis was performed using repeated measurement ANOVA ($F_{(1,3)} = 61.7412$, $p = .0043$). Detailed statistical results are in Supplementary Table S2. Data in the plot is shown as $\bar{x} \pm$ SD. (D) AP arteries and veins in horizontal orientation. Arteries supplying AP reach this area from the caudal and lateral edges (red asterisks). Small vein segments run laterally (arrowheads) from the outer edge of AP, draining to larger veins lying on both sides of AP (white asterisks). These two draining veins converge into a single vein near the caudal corner of the AP (black asterisks). (E) NTS arteries and veins in coronal orientation. The arteries supplying the NTS enter from its lateral and ventral aspects (red asterisks) and the draining veins lie at the lateral aspect (white asterisks). In (A), (B), $z = 100$ μm; in (D), (E), $z = 300$ μm. Color code: Arteries = orange; capillaries = gray; veins = blue. The remainder of the color code and abbreviations as in Figure 4.

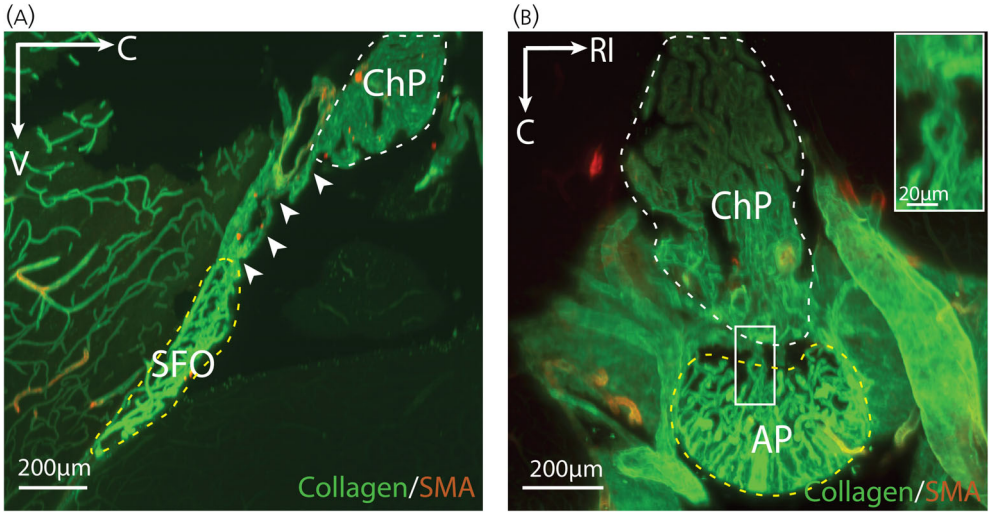

FIGURE 6 SFO and AP Capillary Connection with the ChP. (A) Capillary from the dorsal SFO connects to the vasculature of the ChP (arrowheads) in sagittal orientation. (B) AP capillaries connected to ChP are seen in horizontal orientation. The boxed area is a magnified view of the capillary connection between AP and ChP in the inset. Several capillaries exiting the rostral AP join the capillary vessels of the ChP in the 4V. in Figure 4. In (A) $z = 50$ μm; In (B) $z = 300$ μm. Color coding: Dashed outline of AP and SFO = yellow; ChP = white. Abbreviations are as in Figure 5.

Ji et al.[60] was based on high-level organization such as cortex, cerebellum, hippocampus, hypothalamus, thalamus and striatum; Todorov et al.[63] used finer divisions but did not report analysis results in CVOs; Kirst et al.[61] reported analysis on sensory CVOs but not secretory CVOs. Our studies of the capillary vasculature of sensory CVOs begin to fill these gaps.

For the SFO, the vascular organization seen in our iDISCO material is in good general agreement with the results of prior work on rats and mice. Thus, the primary arterial supply of the SFO is a branch of the cerebral artery entering the SFO from its caudal direction and the SFO is drained by laterally lying septal veins.[64] Densely tangled capillaries intervene between the arterial supply and venous drainage.[65] Our methods extended this early work by enabling the exploration of vascular connections to adjacent neuropil.

The overall vascular organization of AP found in the iDISCO material is also consistent with previous literature. The primary source of AP arteries is the posterior inferior cerebellar artery, which enters the AP from its caudal aspect.[13] The draining vein of AP described by Kroidl in 1968[66] is a "venous semicircle" localized to the caudal portion of 4V, circling the posterior half of the AP, which is also seen in the current study. It finally drains to the basilar vein lying at the ventral medulla. We examined AP's vascular connection with adjacent medulla at a more detailed level, however, here we report findings that differ from the older literature. Roth and Yamamoto[13] reported that the AP and NTS capillaries are joined by connecting portal veins. Their preparation used coronal brain sections and the "connecting vessels" suggested by Roth and Yamamoto are based on sliced sections which obscures the continuity of the BVs in certain orientations. In our 3D reconstruction of the vasculature of this region in the iDISCO material, it is clear that the capillaries of the AP and NTS are interconnected without forming a portal vessel linking the two regions: The capillaries of the two regions are joined, forming a web-like structure seen by viewing the material in various orientations.

4.3 | Characteristics of the vasculature of CVO and their parenchymal attachment sites

It is interesting to note differences in the diameters of capillary vessels in SFO, AP, their portal veins and nearby parenchyma. The general pattern indicates that the portal veins are larger than parenchymal capillaries, and the capillaries in the sensory CVOs are larger than those in the adjacent parenchyma. The difference between the CVO capillaries and their neighboring parenchymal regions is consistent with previous studies, suggesting distinct hemodynamics within different regions.[67] For example, the SFO has a longer blood-dwelling time than its adjacent parenchyma in the capillary lumen and a high blood-to-brain flux rate.[68,69] This is evidenced by comparing the measurements of the amount of radioactive material labeled plasm albumin and diffusible dyes. Albumin in the SFO takes 7–12 times more time to pass through the SFO capillaries compared to blood–brain barrier (BBB) covered capillaries. The radioactive dye is 100–400 times faster to travel across the capillary wall compared to the BBB-covered capillaries. Another example is that AP microcirculation has a significantly larger volume but lower speed of blood flow compared to other regions in the medulla.[68] It is caused by significantly higher resistance in AP capillaries compared to surrounding parenchymal regions.[69] Gross[68] hypothesized that these properties allow AP to have enough time to concentrate the blood-borne signals traveling to its capillaries and for transport to its adjacent medulla.

4.4 | The subregions of SFO and AP have distinct organization

The sensory CVOs have a distinctive vascular organization compared to the surrounding neuropil. Unlike other neuropils, they feature an extensive labyrinth of fenestrated capillaries and large perivascular spaces, features assumed to facilitate communication between the nuclei and their humoral milieu (reviewed in Ref. 6). Within the CVOs, the capillary properties are not homogeneous which gives rise to distinct nuclear subdivisions. The SFO has a ventromedial core which abuts the 3V and a shell region neighboring its rostral parenchyma. The SFO core has larger perivascular spaces than the shell.[70,71] In the most rostral part of the shell, there are no perivascular spaces and no fenestrated capillaries.[68] The AP is divided into a mantle region that lies in direct contact with the 4V, a central zone that is the innermost part of AP and lies directly underneath the mantle region, and a ventral zone that surrounds the medial zone and abuts the adjacent medulla (reviewed in Ref. 15). Unlike the mantle and central zones which bear fenestrated capillaries, the capillaries of the ventral zone are not fenestrated. In addition, the former two zones have clear double-wall capillaries featuring large perivascular space, while the ventral zone shows incomplete fusion of the two walls.[72]

These subdivisional differences indicate that there are some common features of the capillaries in the region forming portal vessels in the SFO and AP. Specifically, there are specialized characteristics of transition zones between the CVOs and their neighboring parenchyma. These zones have little or no perivascular spaces. Also, the capillaries in these zones are less fenestrated than in other subdivisions of the CVOs.[67,71–74] This suggests that the transition zones play a lesser role in the transvascular transportation of blood-borne signals and rather participate in the regulation of intravascular movement of diffusible signals.

4.5 | Implications of joined capillary beds

The discovery of the SFO-posterior septal region portal system and the shared capillary bed of AP and NTS produces a wealth of new research questions, many of which were laid out in the decades that followed the anatomical discovery of a pituitary portal system in 1930,[18] 1933[19] (also reviewed in Ref. 75). In the latter, it took decades to establish the direction of blood flow and in the present cases, we are hesitant to speculate due to the complete absence of evidence. Other open questions include the determination of signals that flow in the joined capillary beds, factors that regulate blood flow, the function of the diffusing signals and mechanism of action at the target sites, etc. Given the unique properties of sensory circumventricular nuclei, including their fenestrated BVs and enlarged perivascular spaces, it will be important to explore how they contribute to or participate in the glymphatic systems of the brain.[4] The answers are vital in understanding the functions and the properties of signals that can be transported from one region to the other within each system.

Knowledge of the possible relationship between SFO and the posterior septal nucleus region is limited. To our knowledge, there is no conclusive evidence of neural connections between SFO and TRS or SFi, and they don't appear to have related functions.[76–78] The SFO is best known for its role in regulating water balance, while SFi and TRS regulate anxiety behavior.[79–81] On the other hand, the AP and NTS are closely related in their functions. As integral parts of the dorsal vagal complex, they regulate cardiovascular functions, feeding behavior and energy balance by integrating peripheral visceral neural inputs, diffusible signals, and afferents from several brain regions.[82,83] The AP seems to be upstream to the NTS, as it sends efferents to the NTS[84] and possibly diffusible signals travel in the same direction.

4.6 | Potential significance of CVO vascular organization

CVOs are conservative structures among vertebrate species.[85] They have morphological and cellular differences among different species, but are thought to have similar structure, organization and primary functions.[14,16] Their close apposition to ventricles suggests that they have an ancient origin. Only recently have CVOs been recognized as an indispensable partner in integrating environmental cues and neural inputs for regulating behaviors.[86] Previous findings suggest that communications among brain regions can be achieved by dual pathways, diffusible routes and neural connections.[10,31]

Together with previous findings of the hypothalamic–pituitary portal axis and the SCN-OVLT portal pathway, the current findings of the SFO-posterior septal nuclei portal system and the shared capillary bed of AP and NTS, suggest that connected capillary networks between morphologically distinct nuclei are a fundamental property of CNS organization. Finally, it is noteworthy that the capillary beds of the SFO and AP are also directly connected to the choroid plexus (Figure 6; also reported in Ref. 16,33,55). Restated, either directly connected or indirectly linked by choroid plexus, the sensory CVOs are all joined together within a single diffusible network with the potential of sharing signaling information between CSF, blood and parenchyma for systemic regulation.

AUTHOR CONTRIBUTIONS

Yifan Yao: Conceptualization; methodology; investigation; visualization; validation; data curation; formal analysis; project administration; writing – review and editing; writing – original draft. **Yannan Chen:** Methodology; software; data curation; investigation; validation; formal analysis; writing – review and editing. **Raju Tomer:** Methodology; software; supervision; resources; writing – review and editing; funding acquisition. **Rae Silver:** Conceptualization; methodology; funding acquisition; investigation; project administration; supervision; resources; writing – original draft; writing – review and editing.

ACKNOWLEDGEMENTS

This work is supported by NSF grant 1749500 and NIH grant R21NS134228 (to R.S.). NIH grant DP2MH119423 (to R.T.). Imaging

was performed with support from the Zuckerman Institute's Cellular Imaging platform, and the National Institute of Health (NIH 1S10OD023587-01).

CONFLICT OF INTEREST STATEMENT

The authors declare no conflicts of interest.

PEER REVIEW

The peer review history for this article is available at https://www.webofscience.com/api/gateway/wos/peer-review/10.1111/jne.13490.

DATA AVAILABILITY STATEMENT

The data that support the findings of this study are available from the corresponding author upon reasonable request.

ORCID

Yifan Yao https://orcid.org/0000-0003-0337-8802
Yannan Chen https://orcid.org/0000-0002-2959-2885

REFERENCES

1. Marcoli M, Agnati LF, Benedetti F, et al. On the role of the extracellular space on the holistic behavior of the brain. *Rev Neurosci*. 2015;26(5):489-506. doi:10.1515/revneuro-2015-0007
2. Iliff JJ, Wang M, Liao Y, et al. A paravascular pathway facilitates CSF flow through the brain parenchyma and the clearance of interstitial solutes, including amyloid β. *Sci Transl Med*. 2012;4(147):147ra111. doi:10.1126/scitranslmed.3003748
3. Bargmann CI, Marder E. From the connectome to brain function. *Nat Methods*. 2013;10(6):483-490. doi:10.1038/nmeth.2451
4. Wardlaw JM, Benveniste H, Nedergaard M, et al. Perivascular spaces in the brain: anatomy, physiology and pathology. *Nat Rev Neurol*. 2020;16(3):137-153. doi:10.1038/s41582-020-0312-z
5. Hablitz LM, Nedergaard M. The glymphatic system: a novel component of fundamental neurobiology. *J Neurosci*. 2021;41(37):7698-7711. doi:10.1523/jneurosci.0619-21.2021
6. Oldfield BJ, McKinley MJ. Chapter 15 – circumventricular organs. In: Paxinos G, ed. *The Rat Nervous System*. 4th ed. Academic Press; 2015:315-333.
7. Gross PM, Weindl A, Knigge KM. Peering through the windows of the brain. *J Cerebral Blood Flow Metab*. 1987;7(6):663-672. doi:10.1038/jcbfm.1987.120
8. Jeong JK, Dow SA, Young CN. Sensory circumventricular organs, neuroendocrine control, and metabolic regulation. *Metabolites*. 2021;11(8):494.
9. Sisó S, Jeffrey M, González L. Sensory circumventricular organs in health and disease. *Acta Neuropathol*. 2010;120(6):689-705. doi:10.1007/s00401-010-0743-5
10. Yao Y, Taub AB, LeSauter J, Silver R. Identification of the suprachiasmatic nucleus venous portal system in the mammalian brain. *Nat Commun*. 2021;12(1):5643. doi:10.1038/s41467-021-25793-z
11. Roy RK, Yao Y, Green IK, et al. Blood flows from the SCN toward the OVLT within a new brain vascular portal pathway. *Sci Adv*. 2024;10(25):eadn8350. doi:10.1126/sciadv.adn8350
12. Akert K. The mammalian subfornical organ. In: Kappers JA, ed. *Neurohormones and Neurohumors: Structure and Function of Regulatory Mechanisms*. Berlin Heidelberg; 1969:78-94.
13. Roth GI, Yamamoto WS. The microcirculation of the area postrema in the rat. *J Comp Neurol*. 1968;133(3):329-340. doi:10.1002/cne.901330304
14. Dellmann HD, Simpson JB. The subfornical organ. In: Bourne GH, Danelli JF, Jeon KW, eds. *International Review of Cytology*. Academic Press; 1979:333-421.
15. McKinley MJ, Clarke IJ, Oldfield BJ. *Circumventricular organs. The Human Nervous System*. 2nd ed. Academic Press; 2003:562-591.
16. Leslie RA. Comparative aspects of the area postrema: fine-structural considerations help to determine its function. *Cell Mol Neurobiol*. 1986;6(2):95-120. doi:10.1007/BF00711065
17. Dorland WAN. *Dorland's Illustrated Medical Dictionary*. 33rd ed. Elsevier; 2020.
18. Popa G. A portal circulation from the pituitary to the hypothalamic region. *J Anat*. 1930;65(Pt 1):88-91.
19. Popa GT, Fielding U. Hypophysio-portal vessels and their colloid accompaniment. *J Anat*. 1933;67(Pt 2):227-232.1.
20. McCann SM, Porter JC. Hypothalamic pituitary stimulating and inhibiting hormones. *Physiol Rev*. 1969;49(2):240-284. doi:10.1152/physrev.1969.49.2.240
21. Herbison AE, Porteous R, Pape J-R, Mora JM, Hurst PR. Gonadotropin-releasing hormone neuron requirements for puberty, ovulation, and fertility. *Endocrinology*. 2008;149(2):597-604. doi:10.1210/en.2007-1139
22. Harris GW. Neural control of the pituitary gland. *Br Med J*. 1955;2(4371):559-564.
23. Ortiga-Carvalho TM, Chiamolera MI, Pazos-Moura CC, Wondisford FE. Hypothalamus-pituitary-thyroid axis. *Compr Physiol*. 2011;6:1387-1428.
24. Perez-Castro C, Renner U, Haedo MR, Stalla GK, Arzt E. Cellular and molecular specificity of pituitary gland physiology. *Physiol Rev*. 2012;92(1):1-38. doi:10.1152/physrev.00003.2011
25. Viau V. Functional cross-talk between the hypothalamic-pituitary-gonadal and -adrenal axes. *J Neuroendocrinol*. 2002;14(6):506-513. doi:10.1046/j.1365-2826.2002.00798.x
26. Ono D, Weaver DR, Hastings MH, Honma K-I, Honma S, Silver R. The suprachiasmatic nucleus at 50: looking back, then looking forward. *J Biol Rhythms*. 2024;39(2):135-165. doi:10.1177/07487304231225706
27. Plant TM. 60 years of neuroendocrinology: the hypothalamo-pituitary–gonadal axis. *J Endocrinol*. 2015;226(2):T41-T54. doi:10.1530/joe-15-0113
28. Dibner C, Schibler U, Albrecht U. The mammalian circadian timing system: organization and coordination of central and peripheral clocks. *Annu Rev Physiol*. 2010;72:517-549. doi:10.1146/annurev-physiol-021909-135821
29. Begemann K, Neumann A-M, Oster H. Regulation and function of extra-SCN circadian oscillators in the brain. *Acta Physiol*. 2020;229(1):e13446. doi:10.1111/apha.13446
30. Starnes AN, Jones JR. Inputs and outputs of the mammalian circadian clock. *Biology*. 2023;12(4):508.
31. Gizowski C, Zaelzer C, Bourque CW. Clock-driven vasopressin neurotransmission mediates anticipatory thirst prior to sleep. *Nature*. 2016;537(7622):685-688. doi:10.1038/nature19756
32. McKinley MJ, Denton DA, Ryan PJ, Yao ST, Stefanidis A, Oldfield BJ. From sensory circumventricular organs to cerebral cortex: neural pathways controlling thirst and hunger. *J Neuroendocrinol*. 2019;31(3):e12689. doi:10.1111/jne.12689
33. Szabó K. The vascular architecture of the developing organum vasculosum of the lamina terminalis (OVLT) in the rat. *Cell Tissue Res*. 1983;233(3):579-592. doi:10.1007/BF00212226
34. Allen Institute for Brain Science. *Allen Mouse Brain Atlas*. Allen Institute for Brain Science; 2004. http://mouse.brain-map.org/
35. Paxinos G, Franklin KBJ. *Paxinos and Franklin's the Mouse Brain in Stereotaxic Coordinates*. 5th ed. Academic Press, an imprint of Elsevier; 2019.
36. Goto M, Oshima I, Tomita T, Ebihara S. Melatonin content of the pineal gland in different mouse strains. *J Pineal Res*. 1989;7(2):195-204. doi:10.1111/j.1600-079X.1989.tb00667.x

37. Renier N, Adams EL, Kirst C, et al. Mapping of brain activity by automated volume analysis of immediate early genes. *Cell*. 2016;165(7):1789–1802.
38. Rogers JH, Résibois A. Calretinin and calbindin-D28k in rat brain: patterns of partial co-localization. *Neuroscience*. 1992;51(4):843-865. doi:10.1016/0306-4522(92)90525-7
39. Watanabe K, Irie K, Hanashima C, Takebayashi H, Sato N. Diencephalic progenitors contribute to the posterior septum through rostral migration along the hippocampal axonal pathway. *Sci Rep*. 2018;8(1):11728. doi:10.1038/s41598-018-30020-9
40. Tomer R, Ye L, Hsueh B, Deisseroth K. Advanced CLARITY for rapid and high-resolution imaging of intact tissues. *Nat Protoc*. 2014;9(7):1682-1697. doi:10.1038/nprot.2014.123
41. Hörl D, Rojas Rusak F, Preusser F, et al. BigStitcher: reconstructing high-resolution image datasets of cleared and expanded samples. *Nat Methods*. 2019;16(9):870-874. doi:10.1038/s41592-019-0501-0
42. Datta MS, Chen Y, Chauhan S, et al. Whole-brain mapping reveals the divergent impact of ketamine on the dopamine system. *Cell Rep*. 2023;42(12):113491. doi:10.1016/j.celrep.2023.113491
43. McCormick M, Liu X, Ibanez L, Jomier J, Marion C. ITK: enabling reproducible research and open science. *Front Neuroinform*. 2014;8:13. doi:10.3389/fninf.2014.00013
44. Schindelin J, Arganda-Carreras I, Frise E, et al. Fiji: an open-source platform for biological-image analysis. *Nat Methods*. 2012;9(7):676-682. doi:10.1038/nmeth.2019
45. Schaeffer S, Iadecola C. Revisiting the neurovascular unit. *Nat Neurosci*. 2021;24(9):1198-1209. doi:10.1038/s41593-021-00904-7
46. Harris CR, Millman KJ, van der Walt SJ, Gommers R, Virtanen P, Cournapeau D. Array programming with NumPy. *Nature*. 2020;585(7825):357-362. doi:10.1038/s41586-020-2649-2
47. McKinney W. Data structures for statistical computing in python. *SciPy*. 2010;445:51-56.
48. Vallat R. Pingouin: statistics in python. *J Open Source Softw*. 2018;3(31):1026. doi:10.21105/joss.01026
49. Hunter JD. Matplotlib: a 2D graphics environment. *Comput Sci Eng*. 2007;9(3):90-95.
50. Waskom ML. Seaborn: statistical data visualization. *J Open Source Softw*. 2021;6(60):3021.
51. Swanson LW, Cowan WM. The connections of the septal region in the rat. *J Comp Neurol*. 1979;186(4):621-655. doi:10.1002/cne.901860408
52. Swanson LW, Risold P-Y. On the basic architecture of the septal region. In: Numan R, ed. *The Behavioral Neuroscience of the Septal Region*. New York; 2000:1-14.
53. Akert K, Potter HD, Anderson JW. The subfornical organ in mammals. I. Comparative and topographical anatomy. *J Comp Neurol*. 1961;116(1):1-13. doi:10.1002/cne.901160102
54. Duvernoy HM, Risold P-Y. The circumventricular organs: an atlas of comparative anatomy and vascularization. *Brain Res Rev*. 2007;56(1):119-147. doi:10.1016/j.brainresrev.2007.06.002
55. Lind RW. Bi-directional, chemically specified neural connections between the subfornical organ and the midbrain raphe system. *Brain Res*. 1986;384(2):250-261. doi:10.1016/0006-8993(86)91161-3
56. Mark MH, Farmer PM. The human subfornical organ: an anatomic and ultrastructural study. *Ann Clin Lab Sci*. 1984;14(6):427-442.
57. Akmayev IG. Morphological aspects of the hypothalamic-hypophyseal system. *Z Zellforsch Mikrosk Anat*. 1971;116(2):178-194. doi:10.1007/BF00331260
58. Satoh H, Inokuchi T, Shimizu M, Obayashi H, Nakashima Y. Ultrastructure of the hypophyseal portal vessel in mature rats SEM and TEM observations. *Kurume Med J*. 1989;36(3):91-94. doi:10.2739/kurumemedj.36.91
59. Di Giovanna AP, Tibo A, Silvestri L, et al. Whole-brain vasculature reconstruction at the single capillary level. *Sci Rep*. 2018;8(1):12573. doi:10.1038/s41598-018-30533-3
60. Ji X, Ferreira T, Friedman B, et al. Brain microvasculature has a common topology with local differences in geometry that match metabolic load. *Neuron*. 2021;109(7):1168-1187.e13. doi:10.1016/j.neuron.2021.02.006
61. Kirst C, Skriabine S, Vieites-Prado A, et al. Mapping the fine-scale organization and plasticity of the brain vasculature. *Cell*. 2020;180(4):780-795.e25. doi:10.1016/j.cell.2020.01.028
62. Miyawaki T, Morikawa S, Susaki EA, et al. Visualization and molecular characterization of whole-brain vascular networks with capillary resolution. *Nat Commun*. 2020;11(1):1104. doi:10.1038/s41467-020-14786-z
63. Todorov MI, Paetzold JC, Schoppe O, et al. Machine learning analysis of whole mouse brain vasculature. *Nat Methods*. 2020;17(4):442-449. doi:10.1038/s41592-020-0792-1
64. Spoerri O. Concerning the vascularization of the subfornical organ of the rat. *Acta Anat*. 1963;54:333-348.
65. Dempsey EW. Fine-structure of the rat's intercolumnar tubercle and its adjacent ependyma and choroid plexus, with especial reference to the appearance of its sinusoidal vessels in experimental argyria. *Exp Neurol*. 1968;22(4):568-589. doi:10.1016/0014-4886(68)90150-7
66. Kroidl R. Die arterielle und venöse Versorgung der Area postrema der Ratte. *Z Zellforsch Mikrosk Anat*. 1968;89(3):430-452. doi:10.1007/BF00319249
67. Shaver SW, Pang JJ, Wall KM, Sposito NM, Gross PM. Subregional topography of capillaries in the dorsal vagal complex of rats: I. Morphometric properties. *J Comp Neurol*. 1991;306(1):73-82. doi:10.1002/cne.902340306
68. Gross PM. Morphology and physiology of capillary systems in subregions of the subfornical organ and area postrema. *Can J Physiol Pharmacol*. 1991;69(7):1010-1025. doi:10.1139/y91-152%M1954559
69. Gross PM, Sposito NM, Pettersen SE, Fenstermacher JD. Differences in function and structure of the capillary endothelium in gray matter, white matter and a circumventricular organ of rat brain. *Blood Vessels*. 1986;23(6):261-270. doi:10.1159/000158652
70. Hicks A-I, Kobrinsky S, Zhou S, Yang J, Prager-Khoutorsky M. Anatomical organization of the rat subfornical organ. *Front Cell Neurosci*. 2021;15:691711. doi:10.3389/fncel.2021.691711
71. Pócsai K, Kálmán M. Glial and perivascular structures in the subfornical organ: distinguishing the shell and core. *J Histochem Cytochem*. 2015;63(5):367-383. doi:10.1369/0022155415575027
72. Kálmán M, Oszwald E, Pócsai K. Three-plane description of astroglial architecture and gliovascular connections of area postrema in rat: long tanycyte connections to other parts of brainstem. *J Comp Neurol*. 2023;531(8):866-887. doi:10.1002/cne.25470
73. Morita S, Furube E, Mannari T, et al. Heterogeneous vascular permeability and alternative diffusion barrier in sensory circumventricular organs of adult mouse brain. *Cell Tissue Res*. 2016;363(2):497-511. doi:10.1007/s00441-015-2207-7
74. Willis CL, Garwood CJ, Ray DE. A size selective vascular barrier in the rat area postrema formed by perivascular macrophages and the extracellular matrix. *Neuroscience*. 2007;150(2):498-509. doi:10.1016/j.neuroscience.2007.09.023
75. Silver R, Yao Y, Roy RK, Stern JE. Parallel trajectories in the discovery of the SCN-OVLT and pituitary portal pathways: legacies of Geoffrey Harris. *J Neuroendocrinol*. 2023;35(9):e13245. doi:10.1111/jne.13245
76. Hernesniemi J, Kawana E, Bruppacher H, Sandri C. Afferent connections of the subfornical organ and of the supraoptic crest. *Acta Anat*. 2008;81(3):321-336. doi:10.1159/000143768
77. Shute CCD, Lewis PR. The ascending cholilnergic reticular systesm: neocortical olfactory and subcorical projections. *Brain*. 1967;90(3):497-520. doi:10.1093/brain/90.3.497
78. Lind R, Johnson A. Subfornical organ-median preoptic connections and drinking and pressor responses to angiotensin II. *J Neurosci*. 1982;2(8):1043-1051. doi:10.1523/jneurosci.02-08-01043.1982

79. Herkenham M, Nauta WJ. Afferent connections of the habenular nuclei in the rat. A horseradish peroxidase study, with a note on the fiber-of-passage problem. *J Comp Neurol*. 1977;173(1):123-146. doi:10.1002/cne.901730107
80. Pesold C, Treit D. Excitotoxic lesions of the septum produce anxiolytic effects in the elevated plus-maze and the shock-probe burying tests. *Physiol Behav*. 1992;52(1):37-47. doi:10.1016/0031-9384(92)90431-Z
81. Sperlágh B, Maglóczky Z, Vizi ES, Freund TF. The triangular septal nucleus as the major source of ATP release in the rat habenula: a combined neurochemical and morphological study. *Neuroscience*. 1998;86(4):1195-1207. doi:10.1016/S0306-4522(98)00026-8
82. Cheng W, Gordian D, Ludwig MQ, Pers TH, Seeley RJ, Myers MG. Hindbrain circuits in the control of eating behaviour and energy balance. *Nat Metab*. 2022;4(7):826-835. doi:10.1038/s42255-022-00606-9
83. Price CJ, Hoyda TD, Ferguson AV. The area postrema: a brain monitor and integrator of systemic autonomic state. *Neuroscientist*. 2008;14(2):182-194. doi:10.1177/1073858407311100
84. Shapiro RE, Miselis RR. The central neural connections of the area postrema of the rat. *J Comp Neurol*. 1985;234(3):344-364. doi:10.1002/cne.902340306
85. Korzh V, Kondrychyn I. Origin and development of circumventricular organs in living vertebrate. *Semin Cell Dev Biol*. 2020;102:13-20. doi:10.1016/j.semcdb.2019.10.010
86. Fong H, Zheng J, Kurrasch D. The structural and functional complexity of the integrative hypothalamus. *Science*. 2023;382(6669):388-394. doi:10.1126/science.adh8488

SUPPORTING INFORMATION

Additional supporting information can be found online in the Supporting Information section at the end of this article.

How to cite this article: Yao Y, Chen Y, Tomer R, Silver R. Capillary connections between sensory circumventricular organs and adjacent parenchyma enable local volume transmission. *J Neuroendocrinol*. 2025;e13490. doi:10.1111/jne.13490